Balancing Ligand Flexibility versus Rigidity for the Stepwise Self-Assembly of M12L24 via M6L12 Metal–Organic Cages

Liu, C.-L.; Bobylev, E.O.; Fu, Y.; Poole III, D.A.; Robeyns, K.; Fustin, C.-A.; Garcia, Y.; Reek, J.N.H.; Singleton, M.L.

DOI
10.1002/chem.202001399

Publication date
2020

Document Version
Final published version

Published in
Chemistry-A European Journal

Supramolecular Chemistry

Balancing Ligand Flexibility versus Rigidity for the Stepwise Self-Assembly of $M_{12}L_{24}$ via M_6L_{12} Metal–Organic Cages

Cui-Lian Liu,[a] Eduard O. Bobylev,[b] Yang Fu,[a] David A. Poole, III,[b] Koen Robeyns,[a] Charles-André Fustin,[a] Yann Garcia,[a] Joost N. H. Reek,[b] and Michael L. Singleton*[a]

Abstract: Non-covalent interactions are important for directing protein folding across multiple intermediates and can even provide access to multiple stable structures with different properties and functions. Herein, we describe an approach for mimicking this behavior in the self-assembly of metal–organic cages. Two ligands, the bend angles of which are controlled by non-covalent interactions and one ligand lacking the above-mentioned interactions, were synthesized and used for self-assembly with Pd^{2+}. As these weak interactions are easily broken, the bend angles have a controlled flexibility giving access to $M_2(\mathbf{L1})_4$, $M_6(\mathbf{L2})_{12}$, and $M_{12}(\mathbf{L2})_{24}$ cages. By controlling the self-assembly conditions this process can be directed in a stepwise fashion. Additionally, the multiple endohedral hydrogen-bonding sites on the ligand were found to play a role in the binding and discrimination of neutral guests.

The last decades have seen significant advances in the development of molecular systems capable of self-assembling into discrete complex structures.[1] Of the reported approaches, metal–ligand coordination based self-assembly has become one of the most widely used.[2] Numerous nano-sized molecular objects have been reported and found to have interesting applications for sensing, catalysis, drug delivery, storage, and molecular recognition, etc.[3] One of the main tenets in the design of these systems is that the size and shape of the final self-assembled structures can to an extent be predicted based on the shape of the ligands and the coordination preferences of the metal.[4] As an example, the most studied metals for self-assembly, Pd^{2+} and Pt^{2+}, form square planar complexes.[5] When combined with rigid, bent, ditopic ligands this leads to metal–organic polyhedra of M_nL_{2n} stoichiometry, where values for n for the thermodynamically most stable species are generally dependent on the bend angle (angle between donor sites) of the ligand and limited to certain values as a result of geometric constraints.[6] By this strategy, numerous self-assembled M_nL_{2n} cages with $n = 2$, 4, 6, 8, 9,12, 24, 30, 48 have been described.[2d,7]

As the number of components involved is generally large, the self-assembly process for even small cages is complex. Multiple factors (examples: counter ion, solvent, etc.) can influence the topology and nuclearity of the self-assembled structures.[8] In the case of $M_{12}L_{24}$ assemblies, studies by the groups of Yoneya,[9] Fujita[9,10] and Hiraoka[11] have highlighted the diversity of the different possible self-assembly pathways on the potential energy landscape leading to the final most stable structure. Several metastable species, notably M_6L_{12}, M_8L_{16}, and M_9L_{18}, have been identified as kinetic intermediates. However, these species typically exist as mixtures and clean formation of single intermediates in the assembly of larger structures is rare,[12] their stability being limited in part due to tension imparted by the rigid ligands being forced to adapt to narrower bend angles. Though less predictable, flexible ditopic ligands, containing for example aliphatic segments, can lead to the formation of multiple structures, with templates being generally required to shift the equilibrium between them.[13] As such, these provide systems that can evolve, both in terms of structure and function, in response to stimuli.[14] Nevertheless, flexible ditopic ligands generally give smaller self-assembled structures and their use for the formation of larger metal–organic cages is limited.[15]

Interestingly, ditopic ligands that have properties in between flexible and rigid have been less explored[16] but could allow multiple large cages to be selectively obtained from a single combination of metal and ligand. Heteroaromatic amide based ligands, such as in Figure 1, can be an interesting candidate for this purpose. These ligands are flexible in the torsion angles around the amides. However, conjugation across the amide leads to a preferred planar structure and dipole-dipole/hydrogen bonding interactions give strong conformational preferences for the curved structures shown. This motif has been widely used for the development of aromatic oligoamide foldamers with highly predictable and stable structures.[17] For metal based self-assembly, ligands of this type have been used for the formation of small Pd_2L_4 cages but never been shown to be applicable for larger structures.[16b–d] As the above interactions should limit the flexibility of the bend angle, we reasoned that large cages could be accessible. Moreover; as

[a] C.-L. Liu, Y. Fu, Dr. K. Robeyns, Prof. Dr. C.-A. Fustin, Prof. Dr. Y. Garcia, Prof. Dr. M. L. Singleton
Institute of Condensed Matter and Nanosciences
Université catholique de Louvain
Place Louis Pasteur 1, Louvain-la-Neuve, 1348 (Belgium)
E-mail: m.singleton@uclouvain.be

[b] E. O. Bobylev, D. A. Poole, III, Prof. Dr. J. N. H. Reek
Van''t Hoff Institute for Molecular Sciences
University of Amsterdam
Science Park 904, Amsterdam 1098 XH (The Netherlands)

Supporting information and the ORCID identification number(s) for the author(s) of this article can be found under:
https://doi.org/10.1002/chem.202001399.

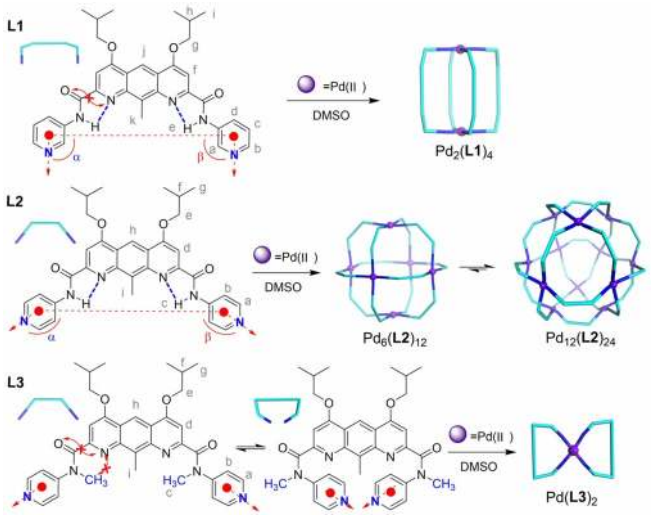

Figure 1. Design of ligands **L1**–**L3**, showing the important non-covalent interactions and the bend angle. Cartoon representations of the products of their self-assembly with Pd^{2+} are shown at the right. The angle between donor atoms on the ligands are calculated as: Bend angle = $(\alpha-90^\circ)+(\beta-90^\circ)$.

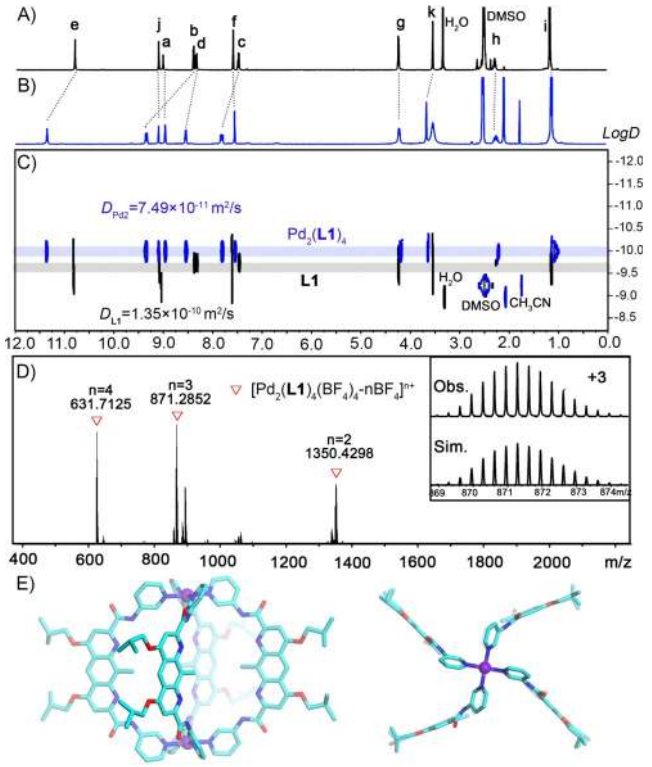

Figure 2. ^{1}H NMR spectra of **L1** (A) and its self-assembly product $Pd_2(\mathbf{L1})_4$ (B). C) An overlay of the DOSY spectra of **L1**, $Pd_2(\mathbf{L1})_4$. All signal assignments correspond to those shown in Figure 1. D) HRMS for $Pd_2(\mathbf{L1})_4$ as its BF_4^- salt. Inset shows the comparison of the observed isotopic pattern with the simulated spectrum. E) X-ray crystal structure of $Pd_2(\mathbf{L1})_4$ with views perpendicular (left) and along (right) the Pd-Pd axis. Protons, solvent molecules and counterions are omitted for clarity.

minor deviations in the torsion angles can lead to an increase in the ligand bend angle, transformation to larger cage structures can potentially be facilitated just by heating; the energetic cost of the less favored conformation being compensated by the additional M–L bonds.

Based on this idea and to study how conformational preferences for the ligand can be used to control self-assembly, we developed ligands **L1–L3**, Figure 1. **L1** and **L2** favor the concave structures because of electrostatic/hydrogen bonding interactions, while **L3** lacks the above-mentioned N-H-N interactions and is expected to be more flexible. The X-ray structures of **L1** and **L2** indeed show the expected curved flat structures. To look at the restriction of the torsion angles around the amides and the flexibility of the ligand, molecular dynamics simulations (See Supporting Information) were used to compare the properties of **L2** to the analogous structure lacking endocyclic nitrogens, **L4**. These indeed show that while the latter is wildly flexible, the two pyridyl moieties in **L2** prefer the conformation observed in the X-ray structure. Still, a range of bend angles is possible, potentially giving access to multiple stable species. This variability can also be seen in the self-assembly of **L1**.

Complexation of **L1** with Pd^{2+} (NO_3^-, BF_4^-, $CF_3SO_3^-$ or PF_6^- salt) in [D_6]DMSO, results in significant shifts of the proton resonances as depicted in the ^{1}H NMR (Figure 2A,B). The formation of a single species was supported by diffusion-ordered ^{1}H NMR (DOSY), Figure 2C, which shows all new signals having the same diffusion coefficient of $D = 7.49\times10^{-11}$ m^2 s^{-1}. The diffusion coefficient in hand, a radius of 13.4 Å can be estimated for the formed system using the Stokes-Einstein-Equation. Figure 2D, HRMS analysis suggests formation of a complex with the formula $Pd_2(\mathbf{L1})_4(BF_4)_4$, based on a series of isotopic pattern corresponding to the loss of two, three, and four BF_4^- counterions.

The composition was further supported by its solid-state structure, Figure 2E. Each of the palladium ions is found in a square planar N_4 coordination environment comprised of four pyridine units. The N-Pd-N bond angles are all between ≈89–91° and the tetrahedral twist is less than 4°, indicating minimal distortion around the metal. The two palladium (II) ions are bridged by four ligands with a metal–metal distance of 13.3 Å. However, the curved structure of the ligands and the *iso*-butoxy side chains result in a larger diameter for the cage. Distances between terminal carbons on the side chains ranged between 22.9–26.7 Å, consistent with the value obtained by ^{1}H DOSY.

Importantly, compared to the crystal of free **L1**, where the bend angle is ≈−36°, the average bend angle has increased to ≈0° in the $Pd_2(\mathbf{L1})_4$ complex. This difference can be partially attributed to distortions of the C-C-N (113° to 116° in complex) and C-N-C (128° to 124° in complex) angles of the amides. However, the pyridine amides are also twisted away from coplanarity with the central diazaanthracene by ≈37–60° further increasing the bend angle. Similar twisting was observed by Gan and co-workers for an analogous complex containing 9-fluorodiazaanthracene units.[16b] These changes show that the bend angle of these ligands can adapt to form well-defined self-assembled structures, at the expense of weakening the non-covalent interactions. The balance between flexibility and

the rigidity imparted by these interactions should have important directing effects for the self-assembly of ligands with larger bend angles, such as **L2**.

To study this, the self-assembly of **L2** with Pd^{2+} (NO_3^-, BF_4^-, $CF_3SO_3^-$ or PF_6^- salt) was followed by ^{1}H NMR. Within ten minutes of mixing **L2** with Pd^{2+} at 75 °C in DMSO, the ligand is converted into a single high symmetry species, Figure 3A,B. Once formed, this species can be kept in solution at room temperature with no discernable change observed over the course of at least several days. ^{1}H DOSY experiments (Figure 3D) on this complex indicate a discrete species with $D = 4.21 \times 10^{-11}$ $m^2 s^{-1}$, corresponding to a radius of 23.8 Å. This size fits within the calculated dimensions of a Pd_6(**L2**)$_{12}$ cage structure ($18.8 < r_{calcd} < 29.2$ Å), vide infra, and is comparable to sizes for M_6L_{12} structures with similar distances between the *N*-donor atoms.[7e] Further evidence for the Pd_6(**L2**)$_{12}$ was obtained by cold-spray ionization mass spectrometry (CSI-MS) on the BF_4^- salt of the compound, Figure 3E. A series of isotopic patterns corresponding to $[Pd_6(\mathbf{L2})_{12}(BF_4)_{12}\text{-}nBF_4]^{n+}$ ($n = 4$–9) were observed which match well with the simulated isotopic spectra.

After continued heating for one hour, Pd_6(**L2**)$_{12}$ remains the major species in solution by ^{1}H NMR, however a new set of signals starts to appear. These become the major species over the course of four hours giving a spectra with a single set of signals, suggesting the formation of a large symmetric structure,

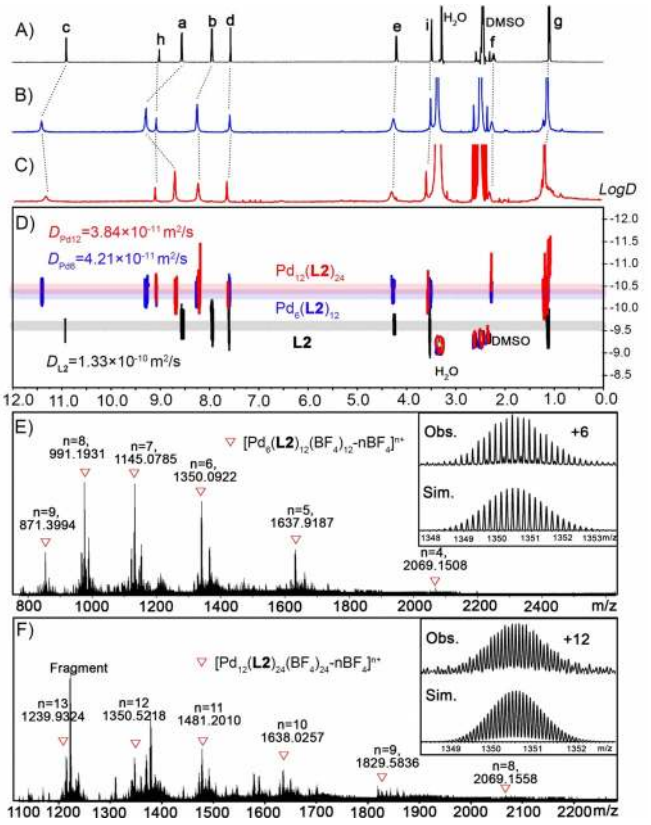

Figure 3. ^{1}H NMR spectra of A) **L2**, B) Pd_6(**L2**)$_{12}$, and C) Pd_{12}(**L2**)$_{24}$. D) An overlay of the DOSY spectra of **L2**, Pd_6(**L2**)$_{12}$ and Pd_{12}(**L2**)$_{24}$. Corresponding average diffusion coefficients are shown. E) Portion of the UHR CSI-MS for Pd_6(**L2**)$_{12}$, and F) Pd_{12}(**L2**)$_{24}$ as their BF_4^- salts. Insets show the comparison of the observed isotopic bundles with the simulated spectra.

Figure 3C. When this change is followed by CSI-MS, the signals for Pd_6(**L2**)$_{12}$ disappear and are replaced by a series of isotopic patterns corresponding to $[Pd_{12}(\mathbf{L2})_{24}(BF_4)_{24-n}BF_4]^{n+}$ ($n = 8$–13), Figure 3F. Consistent with this, a single diffusion band ($D = 3.84 \times 10^{-11}$ $m^2 s^{-1}$) is seen in the ^{1}H DOSY spectrum indicating an object with a larger radius (26.4 Å) than the M_6L_{12} species, which based on the CSI-MS results is assigned to Pd_{12}(**L2**)$_{24}$.

As the components of the solution are not changed and the self-assembly occurs with a range of counterions, the step-wise process may be rationalized based on the conformational control of the ligand. The para relationship in the amino-pyridine groups in **L2** results in an average free ligand bend angle of ≈82°, based on the X-ray structure. This value should favor formation of the observed M_6L_{12} cage.[7e] However, a 30° increase, as observed with **L1**, can permit the formation of the $M_{12}L_{24}$ cage.[7f] While the latter should ultimately be thermodynamically favored,[10b] a significant distortion from the preferred conformation of the ligand is needed. By contrast, the narrower angle needed for the former should be more easily accessible and the formed M_6L_{12} structure should further benefit from stronger intraligand non-covalent interactions. For both cages, the control of the ligand conformation by the non-covalent interactions is important. In **L3**, where the amide proton is replaced by a methyl group, the increased flexibility does not permit the formation of the larger structures. Rather, self-assembly with Pd^{2+} under all conditions gave the mononuclear Pd(**L3**)$_2$, see Supporting Information.

In order to look at changes in the ligands in the M_6L_{12} and $M_{12}L_{24}$ complexes, theoretical calculations at the semi-empirical PM6 level using Gaussian 09 were employed.[18] The computed structures obtained for **L1**, **L2**, and Pd_2(**L1**)$_4$ agree well with the structures determined by X-ray diffraction. The geometry-optimized structures proposed for Pd_6(**L2**)$_{12}$ and Pd_{12}(**L2**)$_{24}$, Figure 4B,C, show highly symmetric assemblies with radii of 22 and 29 Å respectively, within range of the values determined from the ^{1}H DOSY studies. Relative to the calculated structure of free **L2**, noticeable distortions are present in both cages. First, the average bend angles have increased to 97° and 120° for Pd_6(**L2**)$_{12}$ and Pd_{12}(**L2**)$_{24}$ respectively. Unlike Pd_2(**L1**)$_4$, the calculated C-C-N and C-N-C angles show only modest changes between the M_6L_{12} and $M_{12}L_{24}$ cages (114.8° vs. 115.2° for C-C-N and 125.5° vs. 124.7° for C-N-C). The difference in bend angle appears to result primarily from twisting of the pyridine amides. Average torsion angles between the amides and the central aromatic units for the Pd_6(**L2**)$_{12}$ and Pd_{12}(**L2**)$_{24}$ structures are 36° and 55° respectively, versus an angle of nearly 0° in **L2**. For the free ligand, the observed coplanar conformation results from a combination of conjugation and dipole-dipole interactions. Deviation from this conformation to reach the larger bend angles should thus entail a weakening of these interactions. This can be seen in the intraligand hydrogen bonding, where the longer NH···N distance and smaller NH…N angle calculated for Pd_{12}(**L2**)$_{24}$ (2.67 Å) versus Pd_6(**L2**)$_{12}$ (2.48 Å) would be consistent with a weaker interaction. Conversely, the narrower ligand bend angle in Pd_6(**L2**)$_{12}$ allows stronger intraligand interactions, which should help stabilize this intermediate during self-assembly.

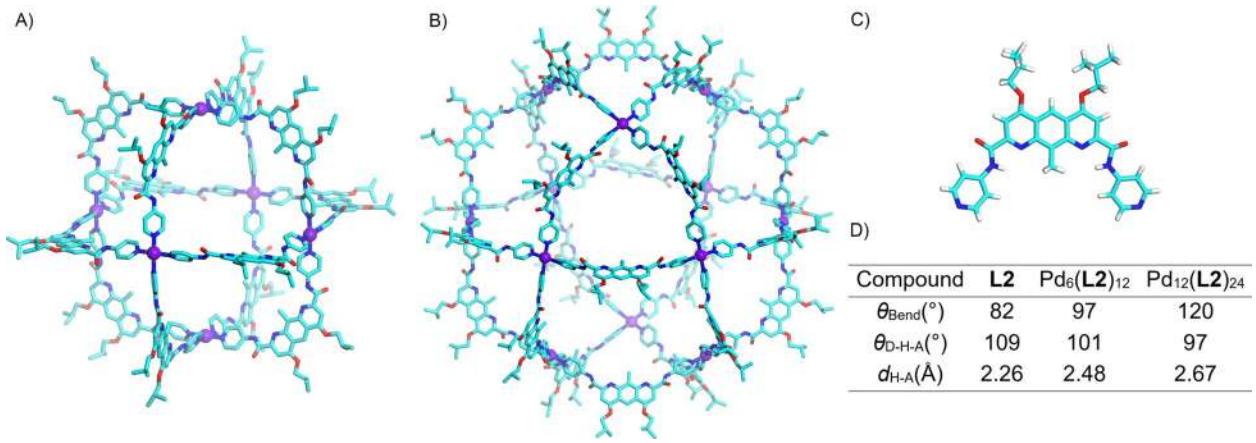

Compound	**L2**	Pd_6(**L2**)$_{12}$	Pd_{12}(**L2**)$_{24}$
θ_{Bend}(°)	82	97	120
$\theta_{D\text{-}H\text{-}A}$(°)	109	101	97
$d_{H\text{-}A}$(Å)	2.26	2.48	2.67

Figure 4. Computationally (PM6) optimized structures for (A) Pd_6**L2**$)_{12}$, (B) Pd_{12}(**L2**$)_{24}$ and (C) the crystal structure of **L2**. Protons in cages are omitted for clarity. D) Comparison of the bend angle and relevant intraligand hydrogen bonding geometric parameters for the structure of free **L2** versus in the ligands of the calculated structures of the M_6L_{12} and $M_{12}L_{24}$ cages.

Of note, during the self-assembly with **L2** a decrease in signal intensity was observed in the NMR upon going from M_6L_{12} to $M_{12}L_{24}$. Using methylsulfone as an internal standard showed that, while for Pd_2(**L1**$)_4$ the ^{1}H NMR signals represent >90% of the initial ligand concentration, for Pd_6(**L2**$)_{12}$ and Pd_{12}(**L2**$)_{24}$ the signals correspond to 51% and 13% respectively. As no precipitation was observed, this was postulated to be due to aggregation of the complexes, a phenomenon previously observed with some metal organic cages.[19] Indeed, dynamic light scattering (DLS) measurements on solutions of Pd_2(**L1**$)_4$, Pd_6(**L2**$)_{12}$ and Pd_{12}(**L2**$)_{24}$ indicated the presence of well-defined particles with hydrodynamic radii of 63–85 nm, see the Supporting Information. For Pd_{12}(**L2**$)_{24}$, this was further confirmed by SEM analysis which found spherical particles with sizes consistent with radii determined by DLS. For the other two complexes, no particles were observed by SEM. This could be due to the lower concentration of the aggregates as indicated in the NMR. Additionally, the lower value of scattered light intensity (I/I_0) in the DLS studies of Pd_6(**L2**$)_{12}$ suggest that the aggregates are present in small quantity in this sample. Variable temperature NMR studies suggest that the aggregates are quite stable. Heating a DMSO sample of Pd_{12}(**L2**$)_{24}$ gives a minor increase in intensity for the signals corresponding to the cage at 80 °C. Nevertheless, this still only accounts for around 21% of the total ligand concentration, indicating only slight disaggregation. Similar results were obtained by variable temperature DLS studies.

In addition to their structural role, the endohedral functionalization by the groups on the ligands can potentially assist in the binding and discrimination of guests. Indeed, the amides appear to interact with the included solvent molecules in the crystal structure of Pd_2(**L1**$)_4$. While, metal–organic cages have been widely exploited for host-guest chemistry, binding neutral guests in polar solvents is still challenging due to competition with counterions and favorable solvation of the guests.[20] To look at the guest binding ability of the aromatic amides cages, we performed preliminary studies on the interaction of neutral guests pyromellitic diimide (**G1**) and pyromellitic dianhydride (**G2**) with the Pd_2(**L1**$)_4$ cage, Figure 5. Both guests are highly soluble in DMSO. Addition of **G1** to a solution of Pd_2(**L1**$)_4$ cage in [D_6]DMSO, resulted in obvious shifts in the proton resonances of the cage, including a noticeable upfield shift for the amide N–H and methyl resonances. NMR titrations for the host-guest binding suggest an affinity of $\approx 11\ M^{-1}$ in DMSO. Similar association constants in DMSO were reported for other Pd_2L_4 cages with polar nitrile containing guests.[20d] For the interaction between **G1** and the cage, aromatic stacking interactions likely play a role given the shielding observed for the majority of the ligand resonances in the presence of the guest. Still, the different binding between **G1** and **G2** indicates that hydrogen bonding interactions between the guest and the host C–H or N–H groups may also be important. The small downfield shift for the signal at 8.9 ppm suggests an interaction between the guest carbonyls and the 2-position C–H of the pyridines as has been previously observed in other cages.[20]

In summary, we have shown that aromatic amide based ligands are capable of self-assembling with Pd^{2+} to give access

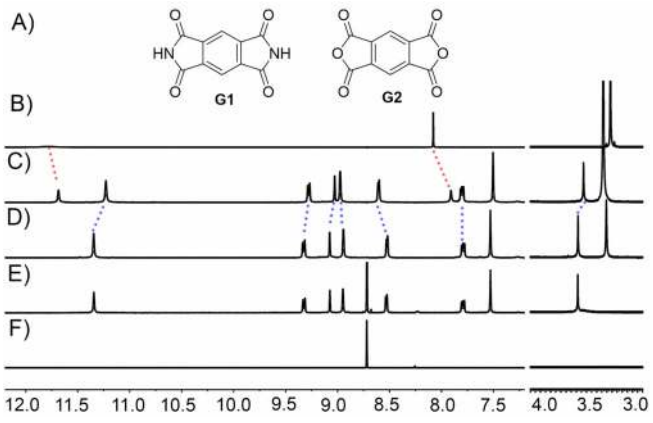

Figure 5. A) Chemical structures of neutral guests **G1** and **G2**, Partial ^{1}H NMR spectra of B) **G1**, C) Pd_2(**L1**$)_4$ + 2.0 equivalent of **G1**, D) Pd_2(**L1**$)_4$, E) Pd_2(**L1**$)_4$ + 4.0 equivalent of **G2** and F) **G2**.

to multiple M_nL_{2n} ($n=2$, 6 and 12) metal–organic cages. The shape of these ligands is stabilized by non-covalent interactions. This bestows a rigidity that allows access to the larger structures, while at the same time permitting a moderate degree of flexibility so that the bend angle can adapt to both the M_6L_{12} and $M_{12}L_{24}$ cages. While the self-assembly of ligand **L2** eventually gives an $M_{12}L_{24}$ cage ($\approx 120^\circ$), the narrower bend angle ($\approx 97^\circ$) in the M_6L_{12} structure can allow for stronger intraligand non-covalent interactions. This can potentially stabilize it as a kinetic intermediate and allow for the unique step-wise self-assembly observed. Preliminary studies with Pd_2(**L1**)$_4$ showed the potential for interaction and discrimination of charge-neutral guests in highly polar solvents. This can be potentially interesting for applications in catalysis. Studies aimed at increasing the interaction with guests and fine-tuning the cage environments are underway and will be reported in due course.

Acknowledgements

This work was supported in part through the Concerted Research Action (ARC16/21-074). C.-L.L. and Y.F were supported by fellowships from the China Scholarship Council. Computational resources have been provided by the supercomputing facilities of the Université catholique de Louvain (CISM/UCL) and the Consortium des équipements de Calcul Intensif en Fédération Wallonie Bruxelles (CPCI) funded by the Fond de la Recherche Scientifique de Belgique (F.R.S.-FNRS) under convention 2.5020.11. We also thank Dr. G. Barozzino for help with NMR measurements.

Conflict of interest

The authors declare no conflict of interest.

Keywords: coordination driven self-assembly · flexible ligands · metal–organic cages · structural transitions · supramolecular chemistry

[1] a) K. Ono, S. Shimo, K. Takahashi, N. Yasuda, H. Uekusa, N. Iwasawa, *Angew. Chem. Int. Ed.* **2018**, *57*, 3113 – 3117; *Angew. Chem.* **2018**, *130*, 3167 – 3171; b) D. Núñez-Villanueva, G. Iadevaia, A. E. Stross, M. A. Jinks, J. A. Swain, C. A. Hunter, *J. Am. Chem. Soc.* **2017**, *139*, 6654 – 6662; c) Q. Luo, C. Hou, Y. Bai, R. Wang, J. Liu, *Chem. Rev.* **2016**, *116*, 13571 – 13632; d) T. Hasell, A. I. Cooper, *Nat.Rev.Mater.* **2016**, *1*, 16053; e) T. R. Cook, P. J. Stang, *Chem. Rev.* **2015**, *115*, 7001 – 7045; f) J. R. Nitschke, *Acc. Chem. Res.* **2007**, *40*, 103 – 112.

[2] a) C. M. Hong, R. G. Bergman, K. N. Raymond, F. D. Toste, *Acc. Chem. Res.* **2018**, *51*, 2447 – 2455; b) S. Datta, M. L. Saha, P. J. Stang, *Acc. Chem. Res.* **2018**, *51*, 2047 – 2063; c) G. H. Clever, P. Punt, *Acc. Chem. Res.* **2017**, *50*, 2233 – 2243; d) D. Fujita, Y. Ueda, S. Sato, N. Mizuno, T. Kumasaka, M. Fujita, *Nature* **2016**, *540*, 563; e) A. M. Castilla, W. J. Ramsay, J. R. Nitschke, *Acc. Chem. Res.* **2014**, *47*, 2063 – 2073.

[3] a) M. Zhang, M. L. Saha, M. Wang, Z. Zhou, B. Song, C. Lu, X. Yan, X. Li, F. Huang, S. Yin, P. J. Stang, *J. Am. Chem. Soc.* **2017**, *139*, 5067 – 5074; b) A. Casini, B. Woods, M. Wenzel, *Inorg. Chem.* **2017**, *56*, 14715 – 14729; c) Q.-Q. Wang, S. Gonell, S. H. A. M. Leenders, M. Dürr, I. Ivanović-Burmazović, J. N. H. Reek, *Nat. Chem.* **2016**, *8*, 225; d) C. J. Brown, F. D. Toste, R. G. Bergman, K. N. Raymond, *Chem. Rev.* **2015**, *115*, 3012 – 3035; e) T. Murase, Y. Nishijima, M. Fujita, *J. Am. Chem. Soc.* **2012**, *134*, 162 – 164; f) J. Wang, C. He, P. Wu, J. Wang, C. Duan, *J. Am. Chem. Soc.* **2011**, *133*, 12402 – 12405; g) P. Mal, B. Breiner, K. Rissanen, J. R. Nitschke, *Science* **2009**, *324*, 1697 – 1699.

[4] a) S. M. Jansze, K. Severin, *J. Am. Chem. Soc.* **2019**, *141*, 815 – 819; b) S. Saha, I. Regeni, G. H. Clever, *Coord. Chem. Rev.* **2018**, *374*, 1 – 14; c) M. Kieffer, B. S. Pilgrim, T. K. Ronson, D. A. Roberts, M. Aleksanyan, J. R. Nitschke, *J. Am. Chem. Soc.* **2016**, *138*, 6813 – 6821; d) H. Yokoyama, Y. Ueda, D. Fujita, S. Sato, M. Fujita, *Chem. Asian J.* **2015**, *10*, 2292 – 2295; e) T. R. Cook, Y.-R. Zheng, P. J. Stang, *Chem. Rev.* **2013**, *113*, 734 – 777.

[5] a) K. Ono, M. Yoshizawa, T. Kato, K. Watanabe, M. Fujita, *Angew. Chem. Int. Ed.* **2007**, *46*, 1803 – 1806; *Angew. Chem.* **2007**, *119*, 1835 – 1838; b) F. Würthner, C.-C. You, C. R. Saha-Möller, *Chem. Soc. Rev.* **2004**, *33*, 133 – 146; c) S. R. Seidel, P. J. Stang, *Acc. Chem. Res.* **2002**, *35*, 972 – 983.

[6] K. Harris, D. Fujita, M. Fujita, *Chem. Commun.* **2013**, *49*, 6703 – 6712.

[7] a) D. Fujita, Y. Ueda, S. Sato, H. Yokoyama, N. Mizuno, T. Kumasaka, M. Fujita, *Chem* **2016**, *1*, 91 – 101; b) D. Fujita, H. Yokoyama, Y. Ueda, S. Sato, M. Fujita, *Angew. Chem. Int. Ed.* **2015**, *54*, 155 – 158; *Angew. Chem.* **2015**, *127*, 157 – 160; c) A. Schmidt, A. Casini, F. E. Kühn, *Coord. Chem. Rev.* **2014**, *275*, 19 – 36; d) Q.-F. Sun, J. Iwasa, D. Ogawa, Y. Ishido, S. Sato, T. Ozeki, Y. Sei, K. Yamaguchi, M. Fujita, *Science* **2010**, *328*, 1144 – 1147; e) K. Suzuki, M. Tominaga, M. Kawano, M. Fujita, *Chem. Commun.* **2009**, 1638 – 1640; f) D. K. Chand, K. Biradha, M. Kawano, S. Sakamoto, K. Yamaguchi, M. Fujita, *Chem. Asian J.* **2006**, *1*, 82 – 90; g) M. Tominaga, K. Suzuki, M. Kawano, T. Kusukawa, T. Ozeki, S. Sakamoto, K. Yamaguchi, M. Fujita, *Angew. Chem. Int. Ed.* **2004**, *43*, 5621 – 5625; *Angew. Chem.* **2004**, *116*, 5739 – 5743.

[8] a) F. J. Rizzuto, P. Pröhm, A. J. Plajer, J. L. Greenfield, J. R. Nitschke, *J. Am. Chem. Soc.* **2019**, *141*, 1707 – 1715; b) T. Zhang, L.-P. Zhou, X.-Q. Guo, L.-X. Cai, Q.-F. Sun, *Nat. Commun.* **2017**, *8*, 15898; c) W. Wang, Y.-X. Wang, H.-B. Yang, *Chem. Soc. Rev.* **2016**, *45*, 2656 – 2693.

[9] M. Yoneya, S. Tsuzuki, T. Yamaguchi, S. Sato, M. Fujita, *ACS Nano* **2014**, *8*, 1290 – 1296.

[10] a) Y. Tachi, S. Sato, M. Yoneya, M. Fujita, Y. Okamoto, *Chem. Phys. Lett.* **2019**, *714*, 185 – 189; b) S. Sato, Y. Ishido, M. Fujita, *J. Am. Chem. Soc.* **2009**, *131*, 6064 – 6065.

[11] S. Kai, T. Shigeta, T. Kojima, S. Hiraoka, *Chem. Asian J.* **2017**, *12*, 3203 – 3207.

[12] a) D. Fujita, A. Takahashi, S. Sato, M. Fujita, *J. Am. Chem. Soc.* **2011**, *133*, 13317 – 13319; b) K.-i. Yamashita, M. Kawano, M. Fujita, *J. Am. Chem. Soc.* **2007**, *129*, 1850 – 1851; c) M. Fujita, F. Ibukuro, K. Yamaguchi, K. Ogura, *J. Am. Chem. Soc.* **1995**, *117*, 4175 – 4176.

[13] a) M. D. Ward, C. A. Hunter, N. H. Williams, *Acc. Chem. Res.* **2018**, *51*, 2073 – 2082; b) J. Mosquera, T. K. Ronson, J. R. Nitschke, *J. Am. Chem. Soc.* **2016**, *138*, 1812 – 1815.

[14] A. J. McConnell, C. S. Wood, P. P. Neelakandan, J. R. Nitschke, *Chem. Rev.* **2015**, *115*, 7729 – 7793.

[15] a) R. A. S. Vasdev, J. A. Findlay, A. L. Garden, J. D. Crowley, *Chem. Commun.* **2019**, *55*, 7506 – 7509; b) M. Han, Y. Luo, B. Damaschke, L. Gómez, X. Ribas, A. Jose, P. Peretzki, M. Seibt, G. H. Clever, *Angew. Chem. Int. Ed.* **2016**, *55*, 445 – 449; *Angew. Chem.* **2016**, *128*, 456 – 460; c) H. S. Sahoo, D. Tripathy, S. Chakrabortty, S. Bhat, A. Kumbhar, D. K. Chand, *Inorg. Chim. Acta* **2013**, *400*, 42 – 50; d) K.-J. Wei, J. Ni, Y. Liu, *Inorg. Chem.* **2010**, *49*, 1834 – 1848; e) J. Xu, K. N. Raymond, *Angew. Chem. Int. Ed.* **2006**, *45*, 6480 – 6485; *Angew. Chem.* **2006**, *118*, 6630 – 6635.

[16] a) S. Pachisia, R. Gupta, *Cryst. Growth Des.* **2019**, *19*, 6039 – 6047; b) Q. Lin, L. Gao, B. Kauffmann, J. Zhang, C. Ma, D. Luo, Q. Gan, *Chem. Commun.* **2018**, *54*, 13447 – 13450; c) N. L. S. Yue, M. C. Jennings, R. J. Puddephatt, *Inorg. Chim. Acta* **2016**, *445*, 37 – 45; d) D. Tripathy, A. K. Pal, G. S. Hanan, D. K. Chand, *Dalton Trans.* **2012**, *41*, 11273 – 11275; e) N. L. S. Yue, M. C. Jennings, R. J. Puddephatt, *Dalton Trans.* **2010**, *39*, 1273 – 1281; f) N. L. S. Yue, D. J. Eisler, M. C. Jennings, R. J. Puddephatt, *Inorg. Chem.* **2004**, *43*, 7671 – 7681; g) Z. Qin, M. C. Jennings, R. J. Puddephatt, *Chem. Commun.* **2002**, 354 – 355.

[17] a) Y. Ferrand, I. Huc, *Acc. Chem. Res.* **2018**, *51*, 970 – 977; b) E. Yashima, N. Ousaka, D. Taura, K. Shimomura, T. Ikai, K. Maeda, *Chem. Rev.* **2016**, *116*, 13752 – 13990; c) D.-W. Zhang, X. Zhao, J.-L. Hou, Z.-T. Li, *Chem. Rev.* **2012**, *112*, 5271 – 5316; d) D. J. Hill, M. J. Mio, R. B. Prince, T. S. Hughes, J. S. Moore, *Chem. Rev.* **2001**, *101*, 3893 – 4012.

[18] Gaussian 09, Revision D.01, M. J. Frisch, G. W. Trucks, H. B. Schlegel, G. E. Scuseria, M. A. Robb, J. R. Cheeseman, G. Scalmani, V. Barone, G. A. Petersson, H. Nakatsuji, X. Li, M. Caricato, A. Marenich, J. Bloino, B. G. Janesko, R. Gomperts, B. Mennucci, H. P. Hratchian, J. V. Ortiz, A. F. Izmaylov, J. L. Sonnenberg, D. Williams-Young, F. Ding, F. Lipparini, F. Egidi, J. Goings, B. Peng, A. Petrone, T. Henderson, D. Ranasinghe, V. G. Zakrzewski, J. Gao, N. Rega, G. Zheng, W. Liang, M. Hada, M. Ehara, K. Toyota, R. Fukuda, J. Hasegawa, M. Ishida, T. Nakajima, Y. Honda, O. Kitao, H. Nakai, T. Vreven, K. Throssell, J. A. Montgomery, Jr., J. E. Peralta, F. Ogliaro, M. Bearpark, J. J. Heyd, E. Brothers, K. N. Kudin, V. N. Staroverov, T. Keith, R. Kobayashi, J. Normand, K. Raghavachari, A. Rendell, J. C. Burant, S. S. Iyengar, J. Tomasi, M. Cossi, J. M. Millam, M. Klene, C. Adamo, R. Cammi, J. W. Ochterski, R. L. Martin, K. Morokuma, O. Farkas, J. B. Foresman, and D. J. Fox, Gaussian, Inc., Wallingford CT, **2016**.

[19] a) H. Li, R. Wang, Y. L. Hong, Z. Liang, Y. Shen, Y. Nishiyama, T. Miyoshi, T. Liu, *Chem. Eur. J.* **2019**, *25*, 5803 – 5808; b) M. Chen, J. Wang, D. Liu, Z. Jiang, Q. Liu, T. Wu, H. Liu, W. Yu, J. Yan, P. Wang, *J. Am. Chem. Soc.* **2018**, *140*, 2555 – 2561; c) W. M. Bloch, J. J. Holstein, B. Dittrich, W. Hiller, G. H. Clever, *Angew. Chem. Int. Ed.* **2018**, *57*, 5534 – 5538; *Angew. Chem.* **2018**, *130*, 5632 – 5637; d) B. Qi, X. Guo, Y. Gao, D. Li, J. Luo, H. Li, S. A. Eghtesadi, C. He, C. Duan, T. Liu, *J. Am. Chem. Soc.* **2017**, *139*, 12020 – 12026; e) H. Li, J. Luo, T. Liu, *Chem. Eur. J.* **2016**, *22*, 17949 – 17952; f) D. Li, W. Zhou, K. Landskron, S. Sato, C. J. Kiely, M. Fujita, T. Liu, *Angew. Chem. Int. Ed.* **2011**, *50*, 5182 – 5187; *Angew. Chem.* **2011**, *123*, 5288 – 5293; g) D. Li, J. Zhang, K. Landskron, T. Liu, *J. Am. Chem. Soc.* **2008**, *130*, 4226 – 4227.

[20] a) F. J. Rizzuto, J. P. Carpenter, J. R. Nitschke, *J. Am. Chem. Soc.* **2019**, *141*, 9087 – 9095; b) T. Y. Kim, R. A. S. Vasdev, D. Preston, J. D. Crowley, *Chem. Eur. J.* **2018**, *24*, 14878 – 14890; c) D. P. August, G. S. Nichol, P. J. Lusby, *Angew. Chem. Int. Ed.* **2016**, *55*, 15022 – 15026; *Angew. Chem.* **2016**, *128*, 15246 – 15250; d) P. Liao, B. W. Langloss, A. M. Johnson, E. R. Knudsen, F. S. Tham, R. R. Julian, R. J. Hooley, *Chem. Commun.* **2010**, *46*, 4932 – 4934; e) T. Kusukawa, M. Fujita, *Angew. Chem. Int. Ed.* **1998**, *37*, 3142 – 3144; *Angew. Chem.* **1998**, *110*, 3327 – 3329.

Manuscript received: March 20, 2020
Accepted manuscript online: May 7, 2020
Version of record online: August 17, 2020